

Self-Organized Criticality in a Stick-Slip Process

Hans Jacob S. Feder and Jens Feder

Department of Physics, University of Oslo, Box 1048, Blindern, 0316 Oslo 3, Norway

(Received 21 January 1991)

The force required to pull sandpaper across a carpet fluctuates. Slips (sudden drops of magnitude M of the force) are observed to have a probability $N(M > m) \sim m^{-b}$ with $b \approx 0.8$. The power spectrum of force fluctuations has a low-frequency $1/f$ behavior. Thus our system reaches a self-organized critical state with fractal scaling in both the spatial and the time domain. We introduce a new *nonconservative* cellular automaton that exhibits self-organized criticality and describes these observations well.

PACS numbers: 91.30.Px, 05.40.+j, 05.45.+b, 05.70.Jk

To describe nature's many caprices a new geometry has evolved. This fractal¹ geometry describes self-similar structures and processes in nature. Examples are mountain landscapes, clouds, coast lines, and irreversible growth structures.^{1,2} But why are fractal structures observed? Bak, Tang, and Wiesenfeld³ found that driven extended dissipative dynamical systems reach a *self-organized critical state* (SOC). They introduced a cellular-automaton (CA) model of a "sandpile" to which grains of sand are continuously added. Their model reached a critical state with a power-law distribution of avalanches and $1/f$ noise in the mass-fluctuation power spectrum. Experiments⁴ show that the existence of the SOC is a finite-size effect for real sandpiles.

Earthquakes have a self-similar distribution of seismic moment m described by the Gutenberg-Richter⁵ power law for the number of quakes above m ,

$$N(M > m) \sim m^{-b}. \quad (1)$$

The value of b is not well established but it is near^{6,7} $b \approx 0.6$ for large earthquakes, and near 0.9 for small ones.⁸ Bak and co-workers suggested^{9,10} that earth-

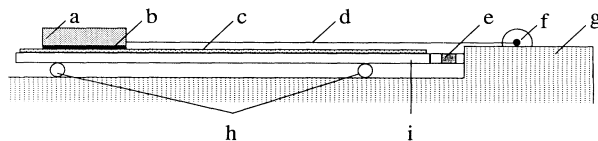


FIG. 1. Experimental setup. The carpet (c) was fixed to a $90 \times 25 \times 0.1$ -cm aluminum plate (i), bent in a \sqcap profile 1.6 cm in height. The edges of the plate rolled on two 10-mm glass tubes (h). The sandpaper (b) was attached to a stiff circular rubber support (a), 125 mm in diameter, and was pulled at a rate of 0.27 mm/s along the carpet by a 0.40-mm nylon fishing line (d) (2 m long) that wound onto a brass cylinder driven by a synchronous motor (f). The force on the carpet was measured using a force transducer (e) (Omega, LCL-010) mounted between the movable aluminum plate and the fixed wooden motor support (g). A voltmeter connected to a PC read the force every at a time $\tau = 0.18$ s with a resolution of $0.2 \mu\text{V}$. A full load of 44.5 N gave a signal of 20 mV.

quake dynamics can be described as a self-organized critical process and introduced CA models of the underlying stick-slip process.¹¹ The model develops into a SOC, but with $b \approx 0.1$. The $1/f$ noise in the time gaps between earthquakes¹² and experimental observation of fractal fault patterns in models of the Earth's crust¹³ further support the idea that earthquakes represent a SOC. Burridge and Knopoff¹¹ did experiments by dragging chains of metal blocks connected by springs along a surface and found that the number of shocks with energy release above m follows Eq. (1) with $b \approx 1$ in their one-dimensional (1D) system. Continuum dynamical models describing systems of masses connected by springs¹⁴⁻¹⁶ also lead to SOC.

We present, for the first time, experimental results on a simple *two-dimensional* stick-slip system (Fig. 1) that exhibits self-organized criticality. The force required to pull a piece of sandpaper across a carpet increases when the sandpaper sticks to the carpet and decreases abruptly when the sandpaper slips (Fig. 2). The power spectrum of the force has $1/f$ noise at low frequencies (Fig. 3), in contrast with the $1/f^2$ behavior observed in sandpiles.⁴ The magnitude of the slips are distributed according to Eq. (1) with $b \approx 0.8$ (Fig. 4).

We also introduce a new *nonconservative* cellular-

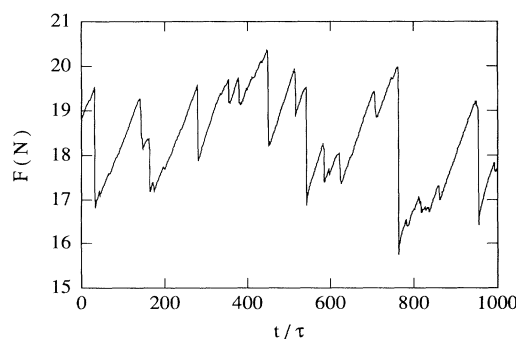


FIG. 2. The force required to pull a 120-grain sandpaper 12.5 cm in diameter across a carpet as a function of reduced time t/τ .

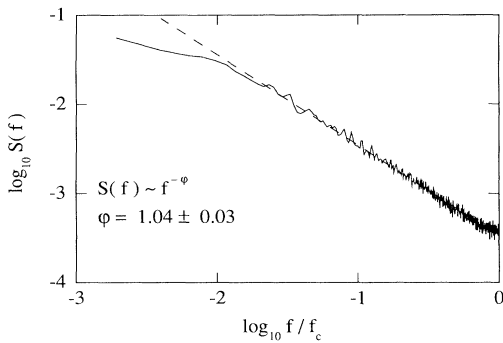


FIG. 3. Power spectrum $S(f)$ (arbitrary units) of force fluctuations as a function of frequency for the experiment for which a part of the time sequence is shown in Fig. 2. The cutoff frequency is $f_c = 2.8$ Hz. The dashed line is a fit to the data of the function $S(f) \sim f^{-\varphi}$.

automaton model that exhibits SOC and may describe our experiments. In noise-driven systems^{17,18} it is believed that the necessary (and sufficient) condition for SOC is that the dynamics satisfy a conservation law. For the models discussed here the conditions under which one should expect SOC are largely unknown.

In our experiments we dragged sandpaper across a carpet. The nylon string stretched elastically when the sandpaper stuck to the carpet. The important attribute of the synthetic carpet used was that it has *loops*. The sandpaper did not stick well to carpets with “hairs.” Individual loops of the carpet also stretched until one or more of them lost their grip. In large slips the sandpaper moved as a whole. In small slips we could not see the motion of the paper but measured and heard that loops lost their grip. The force measured increased with sandpaper diameter and with weight added on top of the moving sandpaper. Coarser-grained sandpaper also resulted in larger forces. We were limited by the maximum load allowed on the force transducer, motor, and

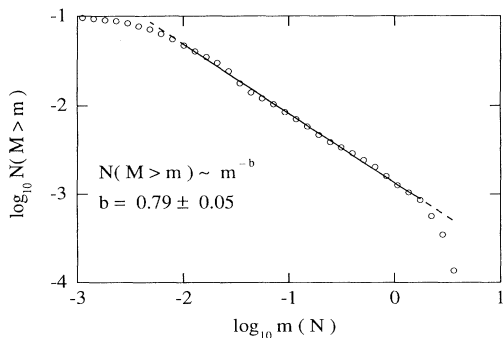


FIG. 4. The probability for having slips of magnitude M above m for the experiment which Fig. 2 is a part of. The straight line is a fit of the function $N(M > m) \sim m^{-b}$ with $b = 0.79 \pm 0.05$ estimated from 6390 slips.

gears and by the sensitivity of the force transducer. We adjusted the load to obtain the highest possible dynamical range for force measurements.

The power spectrum of the force time series is shown in Fig. 3. The results are well described by $S(f) \sim f^{-\varphi}$ for low frequencies. Averaging over many experiments and results on sandpaper 125 and 55 mm in diameter we conclude that the stick-slip process studied has a power-law behavior with a dynamical exponent $\varphi = 1.04 \pm 0.03$.

Our system had complicated elastic properties and boundary conditions. The sandpaper with its support was comparatively stiff. At length scales above the typical loop size the carpet is a low-stiffness quasi-2D elastic medium. Between slips the movement of the sandpaper was due to the *elastic* deformation in the carpet surface. Within the framework of linear elasticity we may give a qualitative argument for the response of our system: At time t and at a position \mathbf{r}' the carpet exerts a force $\mathbf{f}(\mathbf{r}', t)$ on the sandpaper and vice versa. The resulting displacement $\mathbf{u}(\mathbf{r}, t)$ is determined by an elastic response function \mathbf{G} :

$$\mathbf{u}(\mathbf{r}, t) = \int_S d^2r' \mathbf{G}(\mathbf{r} - \mathbf{r}') \cdot \mathbf{f}(\mathbf{r}', t), \quad (2)$$

where S is the sandpaper area. For the sake of argument assume that over some fault area A a slip occurs with a reduction of force $\Delta \mathbf{f}(\mathbf{r}) = \mathbf{f}_{\text{after}} - \mathbf{f}_{\text{before}}$ for $\mathbf{r} \in A$. The average slip ε in the fault is related to the average force change by $\langle \Delta f \rangle = \mu \varepsilon$, through the shear modulus μ . The change in displacements $\Delta \mathbf{u}(\mathbf{r})$ is proportional to $m = \mu \varepsilon A$ everywhere and therefore the displacement of the sandpaper will be $\Delta x \sim A \mathbf{G} \cdot \langle \Delta \mathbf{f} \rangle \sim \mu \varepsilon A$. In our setup this motion relaxes the nylon string and a decrease of the force F was measured even if the fault did not extend to the rim of the sandpaper. Of course, there are intractable force changes outside the fracture area. Nevertheless, in linear elasticity Δx will still be proportional to $m = \mu \varepsilon A$, a quantity termed the *seismic moment*^{6,8} in the discussion of earthquakes.

Experimentally the force is measured at intervals τ and a slip occurs when the force no longer increases at a constant rate. The magnitude of a slip at time t_0 is approximately $F(t_0) - F(t_0 + \tau) = -\tau F'(t_0 + \tau)$ (the vertical drops in Fig. 2). If there were *no* slip, the force would have increased by $F(t_0) - F(t_0 - \tau) = \tau F'(t_0)$, i.e., the increase observed in the previous time interval. The *magnitude* M of each slip in a series of slips is $M = \tau \times [F'(t_0) - F'(t)]$, i.e., the force measured at t , $F(t)$, subtracted from $F(t - \tau)$ incremented by the increase in F expected by stretching the nonslipping loops. Thus a slip, or series of slips, starts at $t = t_0$ whenever $M \geq 0$. We always have a slip when $F' < 0$. A series of slips ends when F' again becomes positive. The observed magnitude M is proportional to the motion Δx of the sandpaper and by Eq. (2) proportional to the “seismic moment” of the slip.

To quantify the magnitude distribution of the slips we

plot in Fig. 4 the probability $N(M > m)$ of slips having a magnitude M above m . For 2 orders of magnitude $N(M > m)$ follows a power law as in (1) with $b = 0.79 \pm 0.05$ estimated from all our experiments. The falloff at large magnitudes is a finite-size effect, since for a given sandpaper size and load there is a maximum in force that may be observed. We are unable to resolve very small slips and find a roll-off at small m . We believe that $b = 0.8$ is an upper bound, since at the finite sandpaper speed used some slips seen as independent events should in fact be combined into slips of a larger magnitude.

The observed exponent $b \approx 0.8$ is below the value $b \approx 1$ found in 1D experiments¹¹ and in simulations¹⁵ with spring-block models. In a 2D spring-block model¹⁴ $b \approx \frac{2}{3}$. Simulations on a 3D spring-breaking model¹⁶ gave $b \approx 0.6$.

Spring-block models are simplistic models of complicated real systems that require massive computer simulations. Cellular-automaton models offer, at the cost of further simplifications, theoretical models capable of SOC that may be studied with limited computer resources. We have extended Bak's model to *nonconservative* systems replacing their cellular automaton by the updating rule^{9,10}

$$\text{if } u_i \geq U_{\text{cr}} \text{ then } \begin{cases} u_i \rightarrow U_{\text{cr}} - 4, \\ u_{\text{nn}} \rightarrow u_{\text{nn}} + 1. \end{cases} \quad (3)$$

Here u_i is the displacement (in arbitrary units and initially random) of the carpet fibers driven by the sandpaper by either elastic or friction forces on lattice site i of the square ($L \times L$) lattice that represents the carpet surface. All u_i increase slowly with time until¹⁹ one reaches the critical value U_{cr} at which the force from the sandpaper loses its grip and u_i is reduced to $U_{\text{cr}} - 4 = 0$ (we use $U_{\text{cr}} = 4$ as in Refs. 9 and 10). This elementary slip process propagates, via \mathbf{G} in Eq. (2), and increases the load and therefore the displacement at four nearest-neighbor (nn) positions to $u_{\text{nn}} + 1$. Now one or more of the nn sites may also become unstable and a slip process (avalanche or "earthquake") involving many sites may occur. The process stops when for all sites $u_i < U_{\text{cr}}$. The model introduced^{9,10} by Bak and co-workers differs from Eq. (3) in that they replace u_i by $u_i - 4$ whenever $u_i \geq 4$, which is a rule that conserves u_i except at the edge of the lattice. As an example, consider the situation where an nn site has a displacement $u_{\text{nn}} = 3.9$. Then the slip at i results in a change $u_{\text{nn}} \rightarrow 4.9$, and in the further evolution of the slip $u_{\text{nn}} \rightarrow 0$ in our model. At this step Bak's conservative model would give $u_{\text{nn}} \rightarrow 0.9$, where we find $u_{\text{nn}} = 0$.

Our rule takes into account the effect that when a loop in the carpet loses its grip not all the force at i is transferred to the neighboring loops. Force is not conserved and the loss $u_i - U_{\text{cr}}$ in u_i is distributed over the

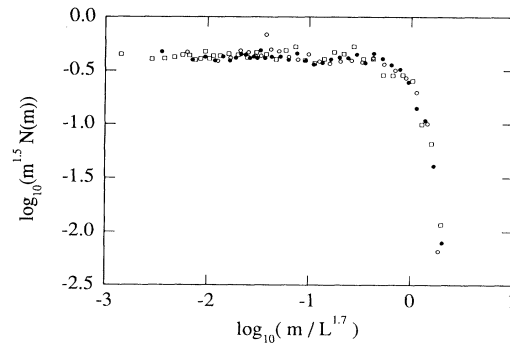


FIG. 5. Scaling plot for probability density for the magnitude m (change in force) of slips in the nonconservative model (3) based on simulations on lattices of size $L \times L$ with $L = 25, 35,$ and 60 (plot symbols, \circ , \square , and \triangle , respectively).

sandpaper by the propagator \mathbf{G} in Eq. (3). The sandpaper moves, stretching all the remaining bonds by a small amount. The magnitude m of a slip is the *change* in total force, $F = \sum u_i$, due to the slip. Our simulations show (Fig. 5) that the probability *density* follows the scaling relation $N(m) = m^{-b-1} g(m/L^\nu)$ with $b \approx 0.5$ and $\nu \approx 1.7$. We also found that the probability density for the number s of sites that take part in a slip follows the same distribution with $b \approx 0.5$ but with $\nu \approx 2.0$. Our model has exponents (b and ν) that differ from those obtained using the conservative model^{9,10} (with $b \approx 0.1$) and it is therefore in a different universality class.²⁰ Our model also exhibits scaling in the time domain but has $S(f) \sim f^{-\varphi}$ with $\varphi \approx 0.9$ only when averaged over many samples since quasiperiodic behavior is observed in individual samples. The introduction of randomness and anisotropy also leads to models with SOC, but with different exponents. A more complete analysis will be published later.

In conclusion, the simple stick-slip process of dragging a sandpaper across a carpet reaches a self-organized critical state characterized by a power-law probability distribution similar to the Gutenberg-Richter law (1) for earthquakes. The power spectrum of the force fluctuations has a $1/f$ behavior at low frequencies. The stick-slip system studied here may represent a simple model of earthquakes. We have introduced a nonconservative cellular-automaton model of stick-slip processes that evolves to SOC with both temporal and spatial power-law correlations that agree better with observations and our experiments than the original conservative CA.

We thank P. Bak and G. Grinstein for sending us preprints and comments and A. Aharony and P. Meakin for stimulating discussions. This work has been supported by VISTA, a research cooperation between the Norwegian Academy of Science and Letters and Den norske stats oljeselskap a.s. (STATOIL).

¹B. B. Mandelbrot, *The Fractal Geometry of Nature* (Free-

man, San Francisco, 1982).

- ²J. Feder, *Fractals* (Plenum, New York, 1988).
- ³P. Bak, C. Tang, and K. Wiesenfeld, *Phys. Rev. Lett.* **59**, 381 (1987); *Phys. Rev. A* **38**, 364 (1988).
- ⁴G. A. Held, D. H. Solina, D. T. Keane, W. J. Haag, P. M. Horn, and G. Grinstein, *Phys. Rev. Lett.* **65**, 1120–1123 (1990).
- ⁵B. Gutenberg and C. F. Richter, *Ann. Geofis.* **9**, 1–15 (1956).
- ⁶H. Kanamori and D. L. Anderson, *Bull. Seismol. Soc. Am.* **65**, 1073–1095 (1975).
- ⁷A. C. Johnston and S. J. Nava, *J. Geophys. Res.* **90**, 6737–6753 (1985).
- ⁸G. Ekström and A. M. Dziewonski, *Nature (London)* **332**, 319–323 (1988).
- ⁹P. Bak and C. Tang, *J. Geophys. Res.* **94**, 15635–15637 (1989).
- ¹⁰P. Bak and K. Chen, in *Fractals and Their Uses in Earth Sciences*, edited by C. C. Barton and P. R. LaPointe (Geological Society of America, Boulder, CO, 1990).
- ¹¹R. Burridge and L. Knopoff, *Bull. Seismol. Soc. Am.* **57**, 341–371 (1967).
- ¹²A. Sornette and D. Sornette, *Europhys. Lett.* **9**, 197–202 (1989).
- ¹³A. Sornette, P. Davy, and D. Sornette, *Phys. Rev. Lett.* **65**, 2266–2269 (1990).
- ¹⁴H. Takayasu and M. Matsuzaki, *Phys. Lett. A* **131**, 244–247 (1988).
- ¹⁵J. M. Carlson and J. S. Langer, *Phys. Rev. Lett.* **62**, 2632 (1989); *Phys. Rev. A* **40**, 6470 (1989).
- ¹⁶K. Chen, P. Bak, and S. P. Obukhov, *Phys. Rev. A* **43**, 625 (1991).
- ¹⁷T. Hwa and M. Kardar, *Phys. Rev. Lett.* **62**, 1813–1816 (1989).
- ¹⁸G. Grinstein, “Generic Scale Invariance in Classical Non-equilibrium Systems,” IBM Research Division, T. J. Watson Research Center, report, 1991 (to be published).
- ¹⁹In any simulation at finite resolution p , the condition $u_i = U_{cr}$ can be tested only to an accuracy of p . In the simulations reported here we chose $p = 2 \times 10^{-5}$, as in Refs. 9 and 10. This step introduces numerical noise into an otherwise deterministic CA.
- ²⁰L. P. Kadanoff, S. R. Nagel, L. Wu, and S. Zhou, *Phys. Rev. A* **39**, 6524–6537 (1989).